# Transverse spin diffusion in strongly interacting Fermi gases

Tilman Enss

*Institut für Theoretische Physik, Universität Heidelberg, D-69120 Heidelberg, Germany*

We compute spin diffusion in a dilute Fermi gas at arbitrary temperature, polarization, and strong interaction in the normal phase using kinetic theory. While the longitudinal spin diffusivity $D_\parallel$ depends weakly on polarization and diverges for small temperatures, the transverse spin diffusivity $D_\perp$ has a strong polarization dependence and approaches a finite value for $T \to 0$ in the Fermi liquid phase. For a 3D unitary Fermi gas at infinite scattering length, the diffusivities reach a minimum near the quantum limit of diffusion $\hbar/m$ in the quantum degenerate regime and are strongly suppressed by medium scattering, and we discuss the importance of the spin-rotation effect. In two dimensions, $D_\perp$ attains a minimum at strong coupling $-1 \lesssim \ln(k_F a_{2D}) \lesssim 1$ and reaches $D_\perp \sim 0.2 \dots 0.3 \hbar/m$ at large polarization. These values are consistent with recent measurements of two-dimensional ultracold atomic gases in the strong coupling regime.

## I. INTRODUCTION

Spin diffusion is one of the basic transport processes which tends to compensate an imbalance of magnetization between regions of a sample. It has been studied, e.g., in liquid helium [1], spintronics [2], and recently in ultracold atomic gases [3,4]. If one writes the local magnetization vector as $\mathcal{M} = \mathcal{M}\hat{e}$, the magnetization gradient $\nabla\mathcal{M} = (\nabla\mathcal{M})\hat{e} + \mathcal{M}\nabla\hat{e}$ has two contributions: longitudinal diffusion acts between regions of different magnitude of magnetization $\mathcal{M}$, i.e., different polarization. Second, transverse spin diffusion arises for spins of the same magnitude $\mathcal{M}$ but different orientation $\hat{e}$, and determines the damping of transverse spin waves. The diffusivities associated with both channels have equal magnitude at high temperatures in the nondegenerate regime (Boltzmann limit), as well as for an unpolarized gas. However, they differ for the most interesting case of a polarized gas at low temperature in the quantum degenerate regime, since different scattering processes are responsible for the two channels. While the longitudinal spin diffusivity $D_\parallel$ grows as $T^{-2}$ for a Fermi liquid at low temperature $T$ due to Pauli blocking, the transverse spin diffusivity $D_\perp$ is much lower—corresponding to larger spin drag—and reaches a constant value as $T \to 0$ in the normal phase, i.e., in the absence of a phase transition.

Experiments in dilute solutions of $^3$He in liquid $^4$He can be understood essentially within kinetic theory and the Born approximation for weakly interacting quasiparticles. Kinetic equations for transverse spin transport were derived by Landau and Silin [5] and applied to degenerate and/or polarized gases [1,6–14]. Transverse diffusion is influenced by the spin-rotation effect by which the spin current precesses around the molecular field of a polarized gas [1]; a similar effect of identical particle spin rotation occurs when two scattering spins rotate around the common axis given by the sum of the two spins [6].

Still, in dilute solutions of $^3$He strong magnetic fields are required to reach a fully polarized state. The advent of ultracold atomic gases [15] provides new experimental opportunities: one can selectively drive radio frequency transitions between atomic hyperfine levels and coherently control the population of different "spin" states. In this way, both longitudinal [3] and transverse [4] spin transport have recently been measured.

Crucially, in ultracold atomic gases the scattering length can be tuned to become much larger than the particle spacing. In such strongly interacting Fermi gases new transport phenomena arise, for instance, almost perfect fluidity [16–18], where the ratio of shear viscosity to entropy density $\eta/s \gtrsim \hbar/k_B$ is bounded from below by quantum mechanics. The related question of whether quantum mechanics provides a bound $D \gtrsim \hbar/m$ for spin diffusion has recently been studied in the normal Fermi liquid phase for longitudinal [3,19–24] and transverse [4] spin diffusion; a sum rule for the spin conductivity is derived in [25]. In current experiments interactions become as strong as allowed by quantum mechanical unitarity, and the Born approximation is not applicable. In this work we develop a kinetic theory based on the *many-body T* matrix, building on previous works using the $T$ matrix [11–13], and we find a substantial suppression of the diffusivity by medium scattering beyond the Born approximation. The values we obtain for the transverse spin diffusivity $D_\perp$ are consistent with the recent spin-echo measurements of a two-dimensional Fermi gas at strong interaction [4].

This paper is organized as follows: In Sec. II we introduce the model of strongly interacting fermions and their scattering in the $T$-matrix approximation, while Sec. III explains the derivation of kinetic theory for transverse and longitudinal spin diffusion. In Sec. IV we present and discuss our results and conclude in Sec. V.

## II. MODEL AND T MATRIX

We consider a two-component Fermi gas with contact interactions described by the grand canonical Hamiltonian,

$$\mathcal{H} = \sum_{\boldsymbol{k}\sigma}(\varepsilon_{\boldsymbol{k}} - \mu_\sigma)c^\dagger_{\boldsymbol{k}\sigma}c_{\boldsymbol{k}\sigma} + \frac{g_0}{V}\sum_{\boldsymbol{k}\boldsymbol{k}'\boldsymbol{q}}c^\dagger_{\boldsymbol{k}+}c^\dagger_{\boldsymbol{k}'-}c_{\boldsymbol{k}'-\boldsymbol{q},-}c_{\boldsymbol{k}+\boldsymbol{q},+},$$

$$(1)$$

with the free-particle dispersion relation $\varepsilon_{\boldsymbol{k}} = \boldsymbol{k}^2/2m$ for particles of mass $m$. We work in units where $\hbar = 1 = k_B$. In a polarized gas the spin species $\sigma = \pm 1$ have different chemical potentials $\mu_\sigma$, and we define the effective magnetic field $h = (\mu_+ - \mu_-)/2$ conjugate to the spin imbalance. Motivated by experiments with ultracold atomic gases, we consider only

$s$-wave scattering, which acts between different spin species by the Pauli principle. The contact interaction $g_0$ needs to be regularized in the ultraviolet both in two and three dimensions, which is done using the $T$ matrix.

### A. Scattering cross sections

In three dimensions (3D) the vacuum, or two-body $T$ matrix, reads

$$\mathcal{T}_0(E) = \frac{4\pi/m}{a^{-1} - \sqrt{-mE}} \tag{2}$$

in terms of the $s$-wave scattering length $a$. In the center-of-mass frame, the kinetic energy of two particles with momenta $\boldsymbol{k}$ and $-\boldsymbol{k}$ is $\omega = 2\varepsilon_{\boldsymbol{k}}$, and $\mathcal{T}_0(\omega + i0) = (4\pi/m)/(a^{-1} + ik)$ is proportional to the Landau scattering amplitude $f(k) = -1/(a^{-1} + ik)$. The differential cross section in vacuum

$$\frac{d\sigma}{d\Omega} = \frac{1}{a^{-2} + k^2} \tag{3}$$

reaches a finite value $a^2$ at low energy $k \to 0$, or diverges as $k^{-2}$ at unitarity $a^{-1} = 0$. At finite density two particles scatter in the presence of a medium which blocks scattering into intermediate states that are already occupied (Pauli blocking), and one has to use the many-body $T$ matrix $\mathcal{T}(\boldsymbol{q},\omega)$ for total momentum $\boldsymbol{q}$ and frequency $\omega$. While the exact $T$ matrix for our model (1) is not known, at sufficiently high temperatures or in a $1/N$ expansion (see below) it is very well approximated by summing up the particle-particle ladder diagrams [26],

$$\mathcal{T}^{-1}(\boldsymbol{q},\omega) = \mathcal{T}_0^{-1}(E = \omega + \mu_+ + \mu_- - \varepsilon_q/2 + i0)$$
$$+ \int \frac{d^d k}{(2\pi)^d} \frac{n_{\boldsymbol{k},+} + n_{\boldsymbol{k}+\boldsymbol{q},-}}{\omega + \mu_+ + \mu_- - \varepsilon_{\boldsymbol{k}} - \varepsilon_{\boldsymbol{k}+\boldsymbol{q}} + i0}, \tag{4}$$

where $n_{\boldsymbol{k}\sigma} = \{\exp[\beta(\varepsilon_{\boldsymbol{k}} - \mu_\sigma)] + 1\}^{-1}$ is the Fermi distribution. In the general case, the scattering cross section is given in terms of the many-body $T$ matrix as

$$\frac{d\sigma}{d\Omega} = \frac{m^2}{(4\pi)^2} |\mathcal{T}(\boldsymbol{q},\omega)|^2, \tag{5}$$

where the kinetic energy is $\omega = \varepsilon_{p_1} + \varepsilon_{p_2} - \mu_+ - \mu_- = \varepsilon_q/2 + 2\varepsilon_{\boldsymbol{k}} - \mu_+ - \mu_-$ for incoming particles with momenta $\boldsymbol{p}_{1,2} = \boldsymbol{q}/2 \pm \boldsymbol{k}$.

In two dimensions (2D) the vacuum $T$ matrix is [27]

$$\mathcal{T}_0(E) = \frac{4\pi/m}{\ln(\varepsilon_B/E) + i\pi}, \tag{6}$$

where $\varepsilon_B \equiv \hbar^2/ma_{2D}^2$ is the binding energy of the two-body bound state. In experiments a quasi-2D geometry is realized by a strong confinement of the three-dimensional system in one direction; well below the confinement energy, $\varepsilon_B$ is replaced by the exact quasi-2D binding energy, which is given in terms of the 3D scattering length $a$ and the confinement length [28]. The $T$ matrix is related to the 2D scattering amplitude in vacuum as $f(k) = m\mathcal{T}_0(2\varepsilon_k + i0) = 4\pi/[\ln(1/k^2 a_{2D}^2) + i\pi]$, and the corresponding differential cross section is

$$\frac{d\sigma}{d\Omega} = \frac{2\pi}{k} \frac{1}{\ln^2\left(k^2 a_{2D}^2\right) + \pi^2}. \tag{7}$$

In the general case of the 2D many-body $T$ matrix (4),

$$\frac{d\sigma}{d\Omega} = \frac{m^2}{8\pi k} |\mathcal{T}(\boldsymbol{q},\omega)|^2. \tag{8}$$

In both 2D and 3D, the scattering cross section does not depend on the orientation of outgoing momenta $\boldsymbol{p}_{3,4} = \boldsymbol{q}/2 \pm \boldsymbol{k}'$; this simplifies the angular averages in the collision integral and precludes lateral spin rotation.

In the Boltzmann limit far above the Fermi temperature $T_F$, the medium corrections are small and one may use the vacuum $T$ matrix. In the quantum degenerate regime, however, medium effects become large, and the system undergoes a phase transition toward $s$-wave superfluidity at $T_c \simeq 0.16\,T_F$ in the 3D unpolarized unitary Fermi gas [29]. In order to include strong coupling effects systematically in a diagrammatic approach, one option is to use a $1/N$ expansion in the number of fermion flavors $N$ to compute the thermodynamics above and below $T_c$ [30] as well as transport [31]. Eventually, the results are extrapolated to the physical case $N = 1$. For large $N$ scattering is weak even at unitarity and it is justified to compute transport properties using kinetic theory consistently up to a certain order in $1/N$; for obtaining transport coefficients to leading order one should use the many-body $T$ matrix in the collision integral but the free Fermi gas for the thermodynamic quantities (pressure, density, susceptibility) that appear in transport [31]. Interaction or mean-field corrections to the quasiparticle dispersion relation as well as to the thermodynamic properties [26] appear only at subleading order in the $1/N$ expansion and are therefore neglected in this work; their importance is discussed, for instance, in Ref. [32].

### B. Thermodynamics

We perform the transport calculation in a grand canonical setting in terms of the dimensionless chemical potentials $\beta\mu_\pm$ and interaction parameter $\beta\varepsilon_B$, where $\beta = 1/k_B T$. In order to compare our results with experiments for a fixed reduced temperature $T/T_F$, magnetic field $h/E_F$, and interaction parameter $k_F a$, one needs to know the equation of state $n(\beta\mu_+, \beta\mu_-, \beta\varepsilon_B)$. For the unpolarized unitary Fermi gas in 3D this has been measured recently [29], but it is not available with comparable accuracy for the polarized gas. We therefore substitute the equation of state of the free Fermi gas, which is readily available and consistent with a $1/N$ expansion. Indeed, at large polarization close to the polaron limit [33,34] where the diffusivity has the most interesting behavior, the majority species behaves almost as a free Fermi gas, and possible phase transitions are shifted to temperatures below the experimentally accessible range ($T \gtrsim 0.1\,T_F$).

The chemical potentials $\mu_\sigma$ for species $\sigma$ determine the fugacities $z_\sigma = \exp(\beta\mu_\sigma)$, and hence the pressure $P_\sigma$, density $n_\sigma$, and susceptibility $\chi_\sigma$ of the free Fermi gas:

$$P_\sigma = -\text{Li}_{d/2+1}(-z_\sigma)\beta^{-1}\lambda_T^{-d}, \tag{9}$$

$$n_\sigma = -\text{Li}_{d/2}(-z_\sigma)\lambda_T^{-d}, \tag{10}$$

$$\chi_\sigma = -\text{Li}_{d/2-1}(-z_\sigma)\beta\lambda_T^{-d}, \tag{11}$$

in terms of the thermal length $\lambda_T = \sqrt{2\pi\beta/m}$ and the polylogarithm $\text{Li}_s(z)$. The (kinetic) energy density

$\varepsilon_\sigma = \int d^d p/(2\pi)^d \, \varepsilon_p n_{p\sigma} = (d/2)P_\sigma$ by scale invariance for the free Fermi gas. The total density $n = n_+ + n_-$ and magnetization $\mathcal{M} = n_+ - n_-$ determine the polarization $M = \mathcal{M}/n$. The characteristic degeneracy temperature is the Fermi temperature $T_F = k_F^2/2m$ associated with the total density of both spin species, $n = k_F^3/3\pi^2$ (3D) and $n = k_F^2/2\pi$ (2D), respectively.

For a typical experimental setup where the reduced temperature $T/T_F$ and the polarization $M$ are given, we first compute the total density as

$$n\lambda_T^3 = \frac{8}{3\sqrt{\pi}}(T/T_F)^{-3/2} \qquad \text{(3D)}, \qquad (12)$$

$$n\lambda_T^2 = 2(T/T_F)^{-1} \qquad \text{(2D)}, \qquad (13)$$

and then the component densities $n_\pm = (1 \pm M)n/2$. Inverting Eq. (10) gives the chemical potentials $\mu_\pm$, which are the starting point for the grand canonical calculation. In two dimensions, $z_\pm = \exp[(1 \pm M)/(T/T_F)] - 1$.

## III. KINETIC THEORY

The kinetic equation for particles with internal states can be written as a matrix equation for the occupation number matrix $\underline{n}_p$ in internal space. In the case of spin-1/2 fermions, $\underline{n}_p$ is a $2 \times 2$ matrix which satisfies the kinetic equation [10]

$$\frac{D\underline{n}_p}{Dt} \equiv \frac{\partial \underline{n}_p}{\partial t} + \frac{1}{2}[\boldsymbol{\nabla}_p\underline{\varepsilon}_p, \boldsymbol{\nabla}_r\underline{n}_p]_+ - \frac{1}{2}[\boldsymbol{\nabla}_r\underline{\varepsilon}_p, \boldsymbol{\nabla}_p\underline{n}_p]_+$$
$$+ \frac{i}{\hbar}[\underline{\varepsilon}_p, \underline{n}_p]_- = \left(\frac{\partial \underline{n}_p}{\partial t}\right)_{\text{coll}}. \qquad (14)$$

The left-hand side is the drift term, where the energy matrix

$$\underline{\varepsilon}_p = \varepsilon_p \underline{I} + \boldsymbol{h}_p \cdot \underline{\boldsymbol{\sigma}} \qquad (15)$$

is given in terms of the bare dispersion relation $\varepsilon_p$ and $\boldsymbol{h}_p = -\frac{1}{2}\hbar\boldsymbol{\Omega}$, where $\boldsymbol{\Omega} = \boldsymbol{\Omega}_0 + \boldsymbol{\Omega}_{\text{mf}}$ is the effective Larmor frequency and $\underline{\boldsymbol{\sigma}}$ are the Pauli matrices. The bare Larmor frequency is $\boldsymbol{\Omega}_0 = \gamma\boldsymbol{B}$ in an external magnetic field $\boldsymbol{B}$, and $\boldsymbol{\Omega}_{\text{mf}}$ is the Larmor frequency due to the molecular field of surrounding spins. The drift term resembles that of the Landau-Silin equation [5], where the anticommutators $[,]_+$ also include mean-field terms and the commutator $[,]_-$ is responsible for the spin-rotation effect of spins precessing about the effective magnetic field. To leading order in a $1/N$ expansion we may neglect the mean-field corrections in the anticommutators because they are small compared to the bare dispersion $\underline{\varepsilon}_p$, but the mean-field term is the leading contribution in the spin-rotation term.

The right-hand side of Eq. (14) is the collision integral

$$\left(\frac{\partial \underline{n}_{p_1}}{\partial t}\right)_{\text{coll}}$$
$$= \frac{1}{(2\pi)^{2d-1}}\int d^d p_2\, d^d p_3\, d^d p_4\, |\mathcal{T}(\boldsymbol{p}_1 + \boldsymbol{p}_2, \omega)|^2$$
$$\times \delta(\boldsymbol{p}_1 + \boldsymbol{p}_2 - \boldsymbol{p}_3 - \boldsymbol{p}_4)\delta(\varepsilon_{p_1} + \varepsilon_{p_2} - \varepsilon_{p_3} - \varepsilon_{p_4})$$
$$\times \frac{1}{4}\{[\underline{\tilde{n}}_1, \underline{\tilde{n}}_2^\pm]_+ \text{Tr}(\underline{n}_3\underline{n}_4^\pm) - [\underline{n}_1, \underline{n}_2^\pm]_+ \text{Tr}(\underline{\tilde{n}}_3\underline{\tilde{n}}_4^\pm)\} \quad (16)$$

for incoming particles $(\boldsymbol{p}_1, +)$ and $(\boldsymbol{p}_2, -)$ and outgoing particles $(\boldsymbol{p}_3, +)$ and $(\boldsymbol{p}_4, -)$. This expression for the collision

integral is identical to Eq. (2.31) of Ref. [12] specialized to fermions and using the fact that the many-body $T$ matrix (4) in the ladder approximation does not depend on the direction of outgoing momenta in the center-of-mass frame. For atomic gases at low temperatures the $s$-wave channel becomes dominant and only scattering between $+$ and $-$ particles occurs; consequently, the $T$ matrix $\mathcal{T}(\boldsymbol{p}_1 + \boldsymbol{p}_2, \omega)$ only has components for unlike spins. This is reflected by the trace over spin indices $\text{Tr}(\underline{n}_3\underline{n}_4^\pm)$, where $\underline{n}_p^\pm = \text{Tr}(\underline{n}_p)\underline{I} - \underline{n}_p$: in $\underline{n}_p^\pm$, the diagonal $+$ and $-$ elements of $\underline{n}_p$ are interchanged, and the trace runs over unlike spins 3 and 4. Furthermore, the fermionic states are unoccupied with probability $\underline{\tilde{n}}_p = \underline{I} - \underline{n}_p$, and the notation $\underline{n}_1$ stands for $\underline{n}_{p_1}$, etc. In the case of longitudinal spin diffusion the collision integral becomes diagonal in the spin indices. However, for transverse spin diffusion the collision integral acquires off-diagonal terms and the full occupation matrix $\underline{n}_p$ needs to be kept.

One may parametrize the occupation matrix $\underline{n}_p$ in terms of particle $f_p$ and spin $\boldsymbol{\sigma}_p$ variables,

$$\underline{n}_p = \frac{1}{2}(f_p\underline{I} + \boldsymbol{\sigma}_p \cdot \underline{\boldsymbol{\sigma}}), \qquad (17)$$

and the kinetic equation (14) may be written in components

$$\frac{Df_p}{Dt} \equiv \frac{\partial f_p}{\partial t} + \sum_i \left[\frac{\partial \varepsilon_p}{\partial p_i}\frac{\partial f_p}{\partial r_i} - \frac{\partial \varepsilon_p}{\partial r_i}\frac{\partial f_p}{\partial p_i} + \frac{\partial \boldsymbol{h}_p}{\partial p_i} \cdot \frac{\partial \boldsymbol{\sigma}_p}{\partial r_i}\right.$$
$$\left. - \frac{\partial \boldsymbol{h}_p}{\partial r_i} \cdot \frac{\partial \boldsymbol{\sigma}_p}{\partial p_i}\right] = \left(\frac{\partial f_p}{\partial t}\right)_{\text{coll}} \qquad (18)$$

and

$$\frac{D\boldsymbol{\sigma}_p}{Dt} \equiv \frac{\partial \boldsymbol{\sigma}_p}{\partial t} + \sum_i \left[\frac{\partial \varepsilon_p}{\partial p_i}\frac{\partial \boldsymbol{\sigma}_p}{\partial r_i} - \frac{\partial \varepsilon_p}{\partial r_i}\frac{\partial \boldsymbol{\sigma}_p}{\partial p_i} + \frac{\partial \boldsymbol{h}_p}{\partial p_i}\frac{\partial f_p}{\partial r_i}\right.$$
$$\left. - \frac{\partial \boldsymbol{h}_p}{\partial r_i}\frac{\partial f_p}{\partial p_i}\right] - \frac{2}{\hbar}\boldsymbol{h}_p \times \boldsymbol{\sigma}_p = \left(\frac{\partial \boldsymbol{\sigma}_p}{\partial t}\right)_{\text{coll}}. \quad (19)$$

The local magnetization is $\boldsymbol{\mathcal{M}}(\boldsymbol{r}, t) = \int d^d p \,\boldsymbol{\sigma}_p/(2\pi)^d = \mathcal{M}(\boldsymbol{r}, t)\hat{\boldsymbol{e}}(\boldsymbol{r}, t)$ and we choose the local magnetization direction $\hat{\boldsymbol{e}}(\boldsymbol{r}, t)$ as the spin quantization axis, such that the local equilibrium distribution matrix $\underline{n}_p^0$ is diagonal with entries $n_{p+}$ and $n_{p-}$. Note that $\boldsymbol{\mathcal{M}}$ need not be parallel to an external magnetic field $\boldsymbol{B}$. According to Eq. (17), $f_p^0 = n_{p+} + n_{p-}$ and $\boldsymbol{\sigma}_p^0 = (n_{p+} - n_{p-})\hat{\boldsymbol{e}}$. The gradient of the magnetization has two contributions, the longitudinal and transverse parts:

$$\frac{\partial \boldsymbol{\mathcal{M}}}{\partial r_i} = \frac{\partial \mathcal{M}}{\partial r_i}\hat{\boldsymbol{e}} + \mathcal{M}\frac{\partial \hat{\boldsymbol{e}}}{\partial r_i}. \qquad (20)$$

We linearize the kinetic equations (18) and (19) around the local equilibrium distribution, $\underline{n}_p = \underline{n}_p^0 + \delta\underline{n}_p$, and write the drift terms as

$$\frac{Df_p}{Dt} \equiv \frac{\partial f_p}{\partial t} - \sum_i v_{pi}\frac{\partial \mathcal{M}}{\partial r_i}\sum_\sigma \sigma t_\sigma \frac{\partial n_{p\sigma}}{\partial \varepsilon_p} = \left(\frac{\partial f_p}{\partial t}\right)_{\text{coll}} \qquad (21)$$

and

$$\frac{D\boldsymbol{\sigma}_p}{Dt} \equiv \frac{\partial \boldsymbol{\sigma}_p}{\partial t} - \sum_i v_{pi}\frac{\partial \mathcal{M}}{\partial r_i}\hat{\boldsymbol{e}}\sum_\sigma t_\sigma \frac{\partial n_{p\sigma}}{\partial \varepsilon_p}$$
$$+ \sum_i v_{pi}\frac{\partial \hat{\boldsymbol{e}}}{\partial r_i}(n_{p+} - n_{p-}) + \boldsymbol{\Omega} \times \boldsymbol{\sigma}_p = \left(\frac{\partial \boldsymbol{\sigma}_p}{\partial t}\right)_{\text{coll}}, \qquad (22)$$

up to corrections of order $\mathcal{O}(\delta \underline{n}_p)$. The second (longitudinal) and third (transverse) terms in Eq. (22) result from the gradient of the local magnetization (20). The derivative $\partial n_{p\sigma}/\partial \varepsilon_p$ in the longitudinal term restricts the momentum integrals in the degenerate regime to a neighborhood of the Fermi surface. In contrast, in the transverse term $n_{p+} - n_{p-}$ is nonzero everywhere between the majority and minority Fermi surfaces; hence the phase space for scattering at low temperature and the transverse scattering rate $\tau_\perp^{-1}$ are larger than in the longitudinal case [7].

In the derivation we have used the Gibbs-Duhem relation $\sum_\sigma n_\sigma (\partial \mu_\sigma / \partial r_i) = 0$ and

$$\frac{\partial n_\sigma}{\partial r_i} = \chi_\sigma \frac{\partial \mu_\sigma}{\partial r_i}, \quad \chi_\sigma = \frac{\partial n_\sigma}{\partial \mu_\sigma}, \tag{23}$$

$$\frac{\partial \mu_\sigma}{\partial r_i} = \sigma t_\sigma \frac{\partial \mathcal{M}}{\partial r_i}, \quad t_\sigma = \frac{1/n_\sigma}{\chi_+/n_+ + \chi_-/n_-}. \tag{24}$$

It then follows that

$$\frac{\partial \varepsilon_p}{\partial p_i} = \frac{p_i}{m} = v_{pi}, \tag{25}$$

$$\frac{\partial f_p^0}{\partial r_i} = -\sum_\sigma \frac{\partial n_{p\sigma}}{\partial \varepsilon_p} \frac{\partial \mu_\sigma}{\partial r_i} = -\frac{\partial \mathcal{M}}{\partial r_i} \sum_\sigma \sigma t_\sigma \frac{\partial n_{p\sigma}}{\partial \varepsilon_p}, \tag{26}$$

$$\frac{\partial \boldsymbol{\sigma}_p^0}{\partial r_i} = \frac{\partial (n_{p+} - n_{p-})}{\partial r_i} \hat{\boldsymbol{e}} + (n_{p+} - n_{p-}) \frac{\partial \hat{\boldsymbol{e}}}{\partial r_i}$$

$$= -\frac{\partial \mathcal{M}}{\partial r_i} \hat{\boldsymbol{e}} \sum_\sigma t_\sigma \frac{\partial n_{p\sigma}}{\partial \varepsilon_p} + \frac{\partial \hat{\boldsymbol{e}}}{\partial r_i}(n_{p+} - n_{p-}), \tag{27}$$

and we have assumed a constant $\boldsymbol{h}_p$.

The particle and spin currents are defined as the velocity weighted by the distribution functions,

$$J_j = \int \frac{d^d p}{(2\pi)^d} v_{pj} f_p, \tag{28}$$

$$\boldsymbol{J}_j = \int \frac{d^d p}{(2\pi)^d} v_{pj} \boldsymbol{\sigma}_p, \tag{29}$$

for a magnetization gradient in direction $j = x, y, z$. We shall not consider the particle current further and instead concentrate on the spin current. The continuity equation for the spin density (magnetization) is

$$\frac{\partial \mathcal{M}}{\partial t} + \sum_j \frac{\partial \boldsymbol{J}_j}{\partial r_j} + \boldsymbol{\Omega}_0 \times \mathcal{M} = 0. \tag{30}$$

The momentum integral over the Boltzmann equation (22) weighted by the velocity $v_{pj}$ yields the time evolution of the spin current,

$$\frac{D\boldsymbol{J}_j}{Dt} \equiv \frac{\partial \boldsymbol{J}_j}{\partial t} + \alpha_\| \frac{\partial \mathcal{M}}{\partial r_j} \hat{\boldsymbol{e}} + \alpha_\perp \mathcal{M} \frac{\partial \hat{\boldsymbol{e}}}{\partial r_j} + (\boldsymbol{\Omega}_0 + \boldsymbol{\Omega}_{\text{mf}}) \times \boldsymbol{J}_j$$

$$= \int \frac{d^d p}{(2\pi)^d} v_{pj} \left( \frac{\partial \boldsymbol{\sigma}_p}{\partial t} \right)_{\text{coll}}, \tag{31}$$

with coefficients

$$\alpha_\| = \int \frac{d^d p}{(2\pi)^d} \sum_i v_{pi} v_{pj} \sum_\sigma t_\sigma \frac{\partial n_{p\sigma}}{\partial \varepsilon_p} = \frac{2/m}{\chi_+/n_+ + \chi_-/n_-}, \tag{32}$$

$$\alpha_\perp = \frac{1}{\mathcal{M}} \int \frac{d^d p}{(2\pi)^d} \sum_i v_{pi} v_{pj} (n_{p+} - n_{p-}) = \frac{P_+ - P_-}{m\mathcal{M}}, \tag{33}$$

for a free Fermi gas. Both $\alpha_\|$ and $\alpha_\perp$ approach $1/m\beta$ in the Boltzmann limit and $n/m\chi$ for the unpolarized gas.

The collision integral on the right-hand side of Eq. (31) determines how the spin current relaxes by collisions, and one has to parametrize the decay by separate time constants $\tau_\|$ and $\tau_\perp$ for longitudinal and transverse relaxation [9],

$$\int \frac{d^d p}{(2\pi)^d} v_{pj} \left( \frac{\partial \boldsymbol{\sigma}_p}{\partial t} \right)_{\text{coll}} = -\frac{1}{\tau_\|} (\boldsymbol{J}_j \cdot \hat{\boldsymbol{e}}) \hat{\boldsymbol{e}} - \frac{1}{\tau_\perp} (\boldsymbol{J}_j \cdot \hat{\boldsymbol{g}}_j) \hat{\boldsymbol{g}}_j. \tag{34}$$

The unit vector

$$\hat{\boldsymbol{g}}_j = x \frac{\partial \hat{\boldsymbol{e}}}{\partial r_j} + y \hat{\boldsymbol{e}} \times \frac{\partial \hat{\boldsymbol{e}}}{\partial r_j} \tag{35}$$

lies in the plane perpendicular to the local magnetization direction $\hat{\boldsymbol{e}}$, at an angle determined by the coefficients $x$ and $y$.

In order to solve Eq. (31), consider first the rotation term $(\boldsymbol{\Omega}_0 + \boldsymbol{\Omega}_{\text{mf}}) \times \boldsymbol{J}_j$, where the molecular field $\boldsymbol{\Omega}_{\text{mf}} = \Omega_{\text{mf}} \hat{\boldsymbol{e}}$ is parallel to the local magnetization $\mathcal{M}$. Hence, $\mathcal{M}$ in Eq. (30) precesses only about the external magnetic field $\boldsymbol{\Omega}_0$ but not about $\boldsymbol{\Omega}_{\text{mf}}$. In contrast, the spin current $\boldsymbol{J}_j$ is in general not parallel to $\mathcal{M}$ and can precess also about the molecular field $\boldsymbol{\Omega}_{\text{mf}}$. It is convenient to work in a frame rotating with the external field $\boldsymbol{\Omega}_0$ in spin space such that the time evolution of $\mathcal{M}$ approaches a quasisteady state [1]. In the same rotating frame, $\partial \boldsymbol{J}_j / \partial t = -\boldsymbol{\Omega}_0 \times \boldsymbol{J}_j$ cancels the free precession of $\boldsymbol{J}_j$ in Eq. (31), but the spin current still precesses about $\boldsymbol{\Omega}_{\text{mf}}$. This causes the spin-rotation effect in transverse diffusion, in contrast to longitudinal diffusion where $\boldsymbol{J}_j \parallel \mathcal{M}$ and spin rotation is absent. Via the continuity equation (30) for the spin density, spin rotation in $\boldsymbol{J}_j$ causes a similar effect in $\mathcal{M}$. Equations (31) and (34) are solved by the spin current [9,12]

$$\boldsymbol{J}_j = -D_\| \frac{\partial \mathcal{M}}{\partial r_j} \hat{\boldsymbol{e}} - \frac{D_\perp^0}{1 + \mu^2} \mathcal{M} \left[ \frac{\partial \hat{\boldsymbol{e}}}{\partial r_j} + \mu \hat{\boldsymbol{e}} \times \frac{\partial \hat{\boldsymbol{e}}}{\partial r_j} \right], \tag{36}$$

with diffusion coefficients $D_\| = \alpha_\| \tau_\|$ and $D_\perp^0 = \alpha_\perp \tau_\perp$. The full transverse diffusion coefficient, including the spin-rotation effect, is given by

$$D_\perp = \frac{D_\perp^0}{1 + \mu^2}, \tag{37}$$

where the spin-rotation parameter

$$\mu = -\Omega_{\text{mf}} \tau_\perp \tag{38}$$

determines how the spin current is rotated in the plane perpendicular to the local magnetization. (This parameter is denoted as $\mu M$ in other works [1,9,12], but we have included the polarization $M$ in the definition of $\mu$.) An example of how the spin-rotation effect lowers the transverse diffusivity

is shown in Sec. IV. Without molecular field there is no spin-rotation effect, $\mu = 0$ and $D_\perp = \alpha_\perp \tau_\perp$.

One may parametrize the deviation from local equilibrium as

$$\delta \underline{n}_p = \tfrac{1}{2}(\delta f_p \, \underline{I} + \delta \boldsymbol{\sigma}_p \cdot \boldsymbol{\sigma}). \tag{39}$$

The deviations $\delta f_p$ and $\delta \boldsymbol{\sigma}_p$ should overlap with the drift terms in Eqs. (21) and (22), and we choose the variational trial functions [9]

$$\delta f_p = c \sum_i v_{pi} \frac{\partial \mathcal{M}}{\partial r_i} \sum_\sigma \sigma t_\sigma \frac{\partial n_{p\sigma}}{\partial \varepsilon_p},$$
$$\delta \boldsymbol{\sigma}_p = \delta \boldsymbol{\sigma}_p^{\parallel} + \delta \boldsymbol{\sigma}_p^{\perp}, \tag{40}$$

with the longitudinal part

$$\delta \boldsymbol{\sigma}_p^{\parallel} = c_{\parallel} \sum_i v_{pi} \frac{\partial \mathcal{M}}{\partial r_i} \hat{\boldsymbol{e}} \sum_\sigma t_\sigma \frac{\partial n_{p\sigma}}{\partial \varepsilon_p} \tag{41}$$

and transverse part

$$\delta \boldsymbol{\sigma}_p^{\perp} = c_\perp \sum_i v_{pi} \hat{\boldsymbol{g}}_i (n_{p+} - n_{p-}). \tag{42}$$

In the following we shall linearize the collision integral (16) for these small deviations from the equilibrium distribution, first in the transverse and then in the longitudinal channel.

Let us briefly discuss the assumptions and approximations involved in the derivation of kinetic theory: we assume (i) applicability of the general hypotheses of Fermi liquid theory and the quasiparticle picture; this condition is met in the normal phase sufficiently far above a possible phase transition to a low-temperature symmetry broken phase; (ii) total spin conservation; (iii) hydrodynamic conditions, i.e., slow variations in time and space; (iv) linearization of the Boltzmann equation, i.e., a small departure from the local equilibrium distribution; (v) ladder approximation for the many-body $T$ matrix (4); consequently, the $T$ matrix does not depend on the direction of outgoing particles in the center-of-mass frame; (vi) no mean-field drift terms except for the spin-rotation term; (vii) the variational ansatz for the deviation from equilibrium, Eqs. (41) and (42); and (viii) no off-energy shell terms in the collision integral [12]. Both the ladder approximation and the absence of mean-field drift terms are justified as the leading order of a low-density expansion [11] or of a systematic $1/N$ expansion in the number of fermion flavors [31]. Once these assumptions are made, the kinetic theory applies to arbitrary temperature from the Boltzmann to the degenerate limit, arbitrary polarization, anisotropic spin-current relaxation times $\tau_{\parallel}$ and $\tau_\perp$, and arbitrary $s$-wave scattering lengths $a$ beyond the Born approximation, as long as the quasiparticle picture remains valid.

Note that the lateral spin-rotation term in the collision integral [6,12] only appears if the $T$ matrix is complex and depends on direction; it vanishes in our case for a direction-independent $T$ matrix, just as it does for a real effective potential [12].

### A. Transverse diffusion

The linearized form of the collision integral (16) for the $T$ matrix (4) differs from the Born approximation in that only

+ and − particles can scatter,

$$\left(\frac{\partial \delta \underline{n}_{p_1}}{\partial t}\right)_{\text{coll}}$$
$$= \frac{1}{(2\pi)^{2d-1}} \int d^d p_2 \, d^d p_3 \, d^d p_4 \, |\mathcal{T}(\boldsymbol{p}_1 + \boldsymbol{p}_2, \omega)|^2$$
$$\times \delta(\boldsymbol{p}_1 + \boldsymbol{p}_2 - \boldsymbol{p}_3 - \boldsymbol{p}_4) \delta(\varepsilon_{p_1} + \varepsilon_{p_2} - \varepsilon_{p_3} - \varepsilon_{p_4})$$
$$\times \tfrac{1}{4} \{ [\delta \underline{\tilde{n}}_2^{\pm} \underline{\tilde{n}}_1 + \underline{\tilde{n}}_2^{\pm} \delta \underline{\tilde{n}}_1 + \underline{\tilde{n}}_1 \delta \underline{\tilde{n}}_2^{\pm} + \delta \underline{\tilde{n}}_1 \underline{\tilde{n}}_2^{\pm}] \operatorname{Tr}(\underline{n}_4^{\pm} \underline{n}_3)$$
$$- [\delta \underline{n}_2^{\pm} \underline{n}_1 + \underline{n}_2^{\pm} \delta \underline{n}_1 + \underline{n}_1 \delta \underline{n}_2^{\pm} + \delta \underline{n}_1 \underline{n}_2^{\pm}] \operatorname{Tr}(\underline{\tilde{n}}_4^{\pm} \underline{\tilde{n}}_3) \}. \tag{43}$$

On the right-hand side a transverse variation of the distribution matrix is inserted using the variational ansatz in Eq. (42):

$$\delta \underline{n}_p^{\perp} = \frac{1}{2} \delta \boldsymbol{\sigma}_p^{\perp} \cdot \boldsymbol{\sigma} = \frac{c_\perp}{2}(n_{p+} - n_{p-}) \sum_i v_{pi} \hat{\boldsymbol{g}}_i \cdot \underline{\boldsymbol{\sigma}}$$
$$= (n_{p+} - n_{p-}) \begin{pmatrix} 0 & s_p^* \\ s_p & 0 \end{pmatrix}, \tag{44}$$

with $s_p = s_{px} + i s_{py}$ and $\boldsymbol{s}_p = (c_\perp / 2)(v_{px} \hat{\boldsymbol{g}}_x + v_{py} \hat{\boldsymbol{g}}_y)$. A typical term in the collision integral (43) has the form [9]

$$\delta \underline{n}_1 \underline{n}_2^{\pm} = (n_{1+} - n_{1-}) \begin{pmatrix} 0 & s_1^* n_{2-} \\ s_1 n_{2+} & 0 \end{pmatrix}, \tag{45}$$

$$[\delta \underline{n}_1, \underline{n}_2^{\pm}]_+ = (n_{1+} - n_{1-})(n_{2+} + n_{2-}) \begin{pmatrix} 0 & s_1^* \\ s_1 & 0 \end{pmatrix}. \tag{46}$$

From $(\delta \underline{n}_p^{\perp})^{\pm} = \operatorname{Tr}(\delta \underline{n}_p^{\perp}) \underline{I} - \delta \underline{n}_p^{\perp}$ follows $\delta \boldsymbol{\sigma}_p^{\perp \pm} = -\delta \boldsymbol{\sigma}_p^{\perp}$, and the matrix product in the curly brackets in Eq. (43) becomes

$$\frac{c_\perp}{2} \sum_i \{ [(\tilde{n}_{1+} - \tilde{n}_{1-})(\tilde{n}_{2+} + \tilde{n}_{2-}) v_{1i} - (\tilde{n}_{1+} + \tilde{n}_{1-})$$
$$\times (\tilde{n}_{2+} - \tilde{n}_{2-}) v_{2i}](n_{3+} n_{4-} + n_{3-} n_{4+}) - [(n_{1+} - n_{1-})$$
$$\times (n_{2+} + n_{2-}) v_{1i} - (n_{1+} + n_{1-})(n_{2+} - n_{2-}) v_{2i}]$$
$$\times (\tilde{n}_{3+} \tilde{n}_{4-} + \tilde{n}_{3-} \tilde{n}_{4+}) \} \hat{\boldsymbol{g}}_i \cdot \underline{\boldsymbol{\sigma}}. \tag{47}$$

Using $\tilde{n}_{1+} \tilde{n}_{2-} n_{3+} n_{4-} = n_{1+} n_{2-} \tilde{n}_{3+} \tilde{n}_{4-}$ from energy conservation and

$$\frac{n_{p+} \tilde{n}_{p-}}{n_{p-} \tilde{n}_{p+}} = \exp(2\beta h), \tag{48}$$

one may rewrite Eq. (47) as

$$-2 c_\perp \sinh(\beta h) \sum_i [e^{-\beta h} n_{1+} n_{2+} + e^{\beta h} n_{1-} n_{2-}]$$
$$\times \tilde{n}_{3+} \tilde{n}_{4-}(v_{1i} - v_{2i}) \hat{\boldsymbol{g}}_i \cdot \underline{\boldsymbol{\sigma}}. \tag{49}$$

The unusual occupation factors $n_{1\pm} n_{2\pm}$ are characteristic of transverse spin diffusion and appear, even though spin is conserved during scattering.

The collision integral determines the relaxation of the transverse current according to Eq. (34) with the variational form (42) also on the right-hand side,

$$\frac{D \boldsymbol{J}_j^{\perp}}{Dt} = \int \frac{d^d p}{(2\pi)^d} v_{pj} \operatorname{Tr} \left[ \underline{\boldsymbol{\sigma}} \left( \frac{\partial \delta \underline{n}_p^{\perp}}{\partial t} \right)_{\text{coll}} \right]$$
$$= -\frac{c_\perp \alpha_\perp \mathcal{M}}{\tau_\perp} \hat{\boldsymbol{g}}_j = -\frac{\boldsymbol{J}_j^{\perp}}{\tau_\perp}, \tag{50}$$

and hence the transverse scattering rate is given by

$$\frac{1}{\tau_\perp} = \frac{\sinh(\beta h)}{\alpha_\perp \mathcal{M}} \frac{1}{(2\pi)^{3d-1}} \int d^d p_1 \dots d^d p_4$$
$$\times \delta(\boldsymbol{p}_1 + \boldsymbol{p}_2 - \boldsymbol{p}_3 - \boldsymbol{p}_4)\,\delta(\varepsilon_{p_1} + \varepsilon_{p_2} - \varepsilon_{p_3} - \varepsilon_{p_4})$$
$$\times |\mathcal{T}(\boldsymbol{p}_1 + \boldsymbol{p}_2,\omega)|^2 \left[e^{-\beta h}n_{1+}n_{2+} + e^{\beta h}n_{1-}n_{2-}\right]$$
$$\times \tilde{n}_{3+}\tilde{n}_{4-}v_{1j}(v_{1j} - v_{2j}). \tag{51}$$

The integral over outgoing momenta yields

$$\frac{1}{\tau_\perp} = \frac{\sinh(\beta h)}{(2\pi)^{2d}\alpha_\perp \mathcal{M}} \int d^d p_1\, d^d p_2\, d\Omega \frac{|\boldsymbol{p}_1 - \boldsymbol{p}_2|}{m} \frac{d\sigma}{d\Omega}$$
$$\times \left[e^{-\beta h}n_{1+}n_{2+} + e^{\beta h}n_{1-}n_{2-}\right]\tilde{n}_{3+}\tilde{n}_{4-}v_{1j}(v_{1j} - v_{2j}), \tag{52}$$

or in center-of-mass coordinates $\boldsymbol{p}_{1,2} = \boldsymbol{q}/2 \pm \boldsymbol{k}$, $\boldsymbol{p}_{3,4} = \boldsymbol{q}/2 \pm \boldsymbol{k}'$,

$$\frac{1}{\tau_\perp} = \frac{\sinh(\beta h)}{(2\pi)^{2d}\alpha_\perp \mathcal{M}} \int d^d q\, d^d k\, d\Omega \frac{2k}{m} \frac{d\sigma}{d\Omega}$$
$$\times \left[e^{-\beta h}n_{1+}n_{2+} + e^{\beta h}n_{1-}n_{2-}\right]\tilde{n}_{3+}\tilde{n}_{4-}\frac{2k_j^2}{m^2}. \tag{53}$$

For $T$-matrix scattering the cross section does not depend on the angle $\Omega$ between $\boldsymbol{k}$ and $\boldsymbol{k}'$, so one can perform the angular integrations explicitly for the Fermi distribution $n_{p\sigma}$ and obtain (no summation over $j$)

$$\int d\Omega_q\, d\Omega_k\, d\Omega \left[e^{-\beta h}n_{1+}n_{2+} + e^{\beta h}n_{1-}n_{2-}\right]$$
$$\times (1 - n_{3+})(1 - n_{4-})k_j^2$$
$$= \frac{S_d^3}{d}k^2[I_{\ell=0}(a - c,b,0) + I_{\ell=0}(a + c,b,0)]I_{\ell=0}(a,b,c), \tag{54}$$

with $a = \beta[\varepsilon_{q/2} + \varepsilon_k - (\mu_+ + \mu_-)/2]$, $b = \beta\sqrt{\varepsilon_q \varepsilon_k}$, $c = \beta h$, and solid angle $S_d$ in $d$ dimensions. The $\ell$-wave angular averages are given by [31]

$$I_\ell = \frac{1}{4}\int_{-1}^{1} dx \frac{P_\ell(x)}{\cosh(a) + \cosh(bx + c)} \quad \text{(3D)}, \tag{55}$$

$$I_\ell = \frac{1}{4\pi}\int_{0}^{2\pi} d\phi \frac{P_\ell(\cos\phi)}{\cosh(a) + \cosh(b\cos\phi + c)} \quad \text{(2D)} \tag{56}$$

with Legendre polynomials $P_\ell(x)$. In three dimensions these integrals are known analytically, in particular,

$$I_{\ell=0}(a,b,c) = \frac{1}{4b\sinh(a)}\ln\frac{\cosh(a + b) + \cosh(c)}{\cosh(a - b) + \cosh(c)}, \tag{57}$$

and analytical expressions involving polylogarithms for $\ell > 0$ [31], while in two dimensions the $I_\ell$ are readily evaluated numerically. This leads to the transverse scattering time

$$\frac{1}{\tau_\perp} = \frac{4S_d^3 \sinh(\beta h)}{d(2\pi)^{2d}m^2(P_+ - P_-)} \int_0^\infty dq\, q^{d-1} \int_0^\infty dk\, k^{d+2}$$
$$\times \frac{d\sigma}{d\Omega}[I_0(a - c,b,0) + I_0(a + c,b,0)]I_0(a,b,c),$$

using $\alpha_\perp$ from Eq. (33). Finally, the diffusion coefficient is given by $D_\perp^0 = \alpha_\perp \tau_\perp$.

## 1. Limiting cases

The expression for the scattering rate simplifies in two limits: the Boltzmann limit $T \gg T_F$ and the unpolarized limit $\beta h \to 0$. In the Boltzmann limit,

$$I_\ell(a,b,c) \to \delta_{\ell,0}\exp(-a), \tag{58}$$

and the angular average $2\sinh(\beta h)[I_0^- + I_0^+]I_0/(P_+ - P_-) \to \beta \lambda_T^{2d} n \exp(-\beta\varepsilon_q/2)\exp(-2\beta\varepsilon_k)$ such that

$$\frac{1}{\tau_\perp} = \frac{2S_d^3 \beta \lambda_T^{2d} n}{d(2\pi)^{2d}m^2} \int_0^\infty dq\, q^{d-1}\exp\left(-q^2\lambda_T^2/8\pi\right)$$
$$\times \int_0^\infty dk\, k^{d+2}\exp\left(-k^2\lambda_T^2/2\pi\right)\frac{d\sigma}{d\Omega}. \tag{59}$$

In the Boltzmann limit the medium effect on scattering becomes small and one may use the vacuum scattering cross section (3), which depends only on the relative momentum $k$ but not on the center-of-mass momentum $q$, and the integrals are readily performed in 3D to yield

$$\frac{1}{\tau_\perp} = \frac{2\sqrt{2}n\lambda_T^7}{3\pi^3 \beta} \int_0^\infty dk\, k^5 \frac{\exp\left(-k^2\lambda_T^2/2\pi\right)}{a^{-2} + k^2}$$
$$= \frac{4\sqrt{2}n\lambda_T^3}{3\pi\beta}[1 - \beta\varepsilon_B - (\beta\varepsilon_B)^2 \exp(\beta\varepsilon_B)\,\text{Ei}(-\beta\varepsilon_B)], \tag{60}$$

where $\text{Ei}(x)$ is the exponential integral, and we have defined a "binding energy" $\varepsilon_B = \hbar^2/ma^2$ also on the BCS side for negative $a$, where there is no two-body bound state. For the unitary gas $\beta\varepsilon_B = 0$ and the expression in brackets is unity, corresponding to an effective cross section $\sigma = \lambda_T^2$, and we obtain the transverse scattering time and diffusivity (with $\alpha_\perp = 1/m\beta$):

$$\tau_\perp = \frac{9\pi^{3/2}\hbar}{32\sqrt{2}k_B T_F}\left(\frac{T}{T_F}\right)^{1/2}, \tag{61}$$

$$D_\perp^0 = \frac{9\pi^{3/2}\hbar}{32\sqrt{2}m}\left(\frac{T}{T_F}\right)^{3/2} \quad \text{(3D)}. \tag{62}$$

These results coincide with the longitudinal scattering time and diffusivity in the Boltzmann limit [3,20]. In the weak-coupling limit the scattering cross section is $4\pi a^2$ and the term in parentheses in Eq. (60) approaches $4\pi a^2/\lambda_T^2$.

In two dimensions we find in the Boltzmann limit

$$\frac{1}{\tau_\perp} = \frac{n\lambda_T^2}{\pi\beta}\lambda_T^4 \int dk\, k^3 \frac{\exp\left(-k^2\lambda_T^2/2\pi\right)}{\ln^2\left(k^2 a_{2D}^2\right) + \pi^2} \tag{63}$$
$$= \frac{2\pi n\lambda_T^2}{\beta Q} = \frac{4\pi k_B T_F}{Q},$$

with

$$Q = \ln^2(2\beta\varepsilon_B/3) + \pi^2 \tag{64}$$

evaluated at the saddle point of the $k$ integral [35]. The scattering time and diffusivity

$$\tau_\perp = \frac{\hbar Q}{4\pi k_B T_F}, \quad D_\perp^0 = \frac{\hbar Q}{4\pi m}\frac{T}{T_F} \quad \text{(2D)} \tag{65}$$

again agree with the longitudinal scattering time and diffusivity in the Boltzmann limit [21,22].

The second limit where $\tau_\perp$ simplifies is the unpolarized limit $\beta h \to 0$ at arbitrary temperature in the normal phase $T > T_c$. The prefactor $\sinh(\beta h)/(P_+ - P_-) \to \beta/n$, and the angular average becomes $[I_0^- + I_0^+]I_0 \to 2I_0^2(a,b,c=0)$:

$$\frac{1}{\tau_\perp} = \frac{8S_d^3\beta}{d(2\pi)^{2d}m^2n} \int dq \, q^{d-1} \int dk \, k^{d+2} \frac{d\sigma}{d\Omega} I_0^2. \quad (66)$$

We shall see below in Sec. III B that this coincides with the longitudinal scattering rate in the unpolarized limit.

### 2. Spin rotation

The transverse diffusivity $D_\perp$ is modified by the spin-rotation effect where the spin current $\boldsymbol{J}_j$ precesses around the molecular field $\boldsymbol{\Omega}_{\rm mf} = \Omega_{\rm mf} \hat{\boldsymbol{e}}$. The field acting on spin 1 due to interaction with surrounding spins 2 reads

$$\boldsymbol{\Omega}_1 = \int \frac{d^d p_2}{(2\pi)^d} \, \mathrm{Re}\, \mathcal{T}(\boldsymbol{p}_1 + \boldsymbol{p}_2, \omega)\boldsymbol{\sigma}_2, \quad (67)$$

with $\omega = \varepsilon_{p_1} + \varepsilon_{p_2} - \mu_+ - \mu_-$. The resulting spin-rotation term in the time evolution of $\boldsymbol{\sigma}_1$ (22) is then

$$\frac{D\boldsymbol{\sigma}_1}{Dt}\bigg|_{\rm spinrot} = \boldsymbol{\Omega}_1 \times \boldsymbol{\sigma}_1$$

$$= \int \frac{d^d p_2}{(2\pi)^d} \, \mathrm{Re}\, \mathcal{T}(\boldsymbol{p}_1 + \boldsymbol{p}_2, \omega)[\boldsymbol{\sigma}_2 \times \boldsymbol{\sigma}_1]. \quad (68)$$

We expand $\boldsymbol{\sigma}_p = \boldsymbol{\sigma}_p^0 + \delta\boldsymbol{\sigma}_p^\perp$ with local equilibrium distribution $\boldsymbol{\sigma}_p^0 = (n_{p+} - n_{p-})\hat{\boldsymbol{e}}$ and small deviation (42) to linear order,

$$\boldsymbol{\sigma}_2 \times \boldsymbol{\sigma}_1 = \boldsymbol{\sigma}_2^0 \times \delta\boldsymbol{\sigma}_1^\perp + \delta\boldsymbol{\sigma}_2^\perp \times \boldsymbol{\sigma}_1^0$$

$$= \sum_i (v_{1i} - v_{2i})(n_{1+} - n_{1-})(n_{2+} - n_{2-})\hat{\boldsymbol{e}} \times \hat{\boldsymbol{g}}_i. \quad (69)$$

The time evolution of the transverse spin current

$$\frac{D\boldsymbol{J}_j^\perp}{Dt}\bigg|_{\rm spinrot} = \int \frac{d^d p_1}{(2\pi)^d} v_{1j} \frac{D\boldsymbol{\sigma}_1}{Dt}\bigg|_{\rm spinrot} \quad (70)$$

can then be written using $[\boldsymbol{J}_j^\perp = c_\perp \alpha_\perp \mathcal{M}\hat{\boldsymbol{g}}_j$ from Eq. (50) as

$$\frac{D\boldsymbol{J}_j^\perp}{Dt}\bigg|_{\rm spinrot} = \Omega_{\rm mf}\, \hat{\boldsymbol{e}} \times \boldsymbol{J}_j^\perp. \quad (71)$$

The spin current precesses around the molecular field with frequency [12]

$$\Omega_{\rm mf} = \frac{1}{\alpha_\perp \mathcal{M}} \int \frac{d^d p_1}{(2\pi)^d} \frac{d^d p_2}{(2\pi)^d} v_{1j}(v_{1j} - v_{2j})(n_{1+} - n_{1-})$$

$$\times (n_{2+} - n_{2-})\,\mathrm{Re}\,\mathcal{T}(\boldsymbol{p}_1 + \boldsymbol{p}_2, \omega), \quad (72)$$

which then determines the spin-rotation parameter $\mu = -\Omega_{\rm mf}\tau_\perp$. For a momentum-independent interaction $\mathrm{Re}\,\mathcal{T} = 2V_0$ this reduces to $\Omega_{\rm mf} = 2V_0\mathcal{M}/\hbar$ [9].

### B. Longitudinal diffusion

For longitudinal spin diffusion one may linearize the distribution matrix with a variation (41) that remains diagonal in the spin indices. Then also the linearized collision integral (16)

is diagonal, and following the standard derivation one obtains the longitudinal scattering rate [8,20–22]:

$$\frac{1}{\tau_\parallel} = \frac{2\beta n}{(2\pi)^{2d}m^2 n_+ n_-} \int d^d q \, d^d k \, d\Omega \, k \frac{d\sigma}{d\Omega}$$

$$\times n_{1+}n_{2-}\tilde{n}_{3+}\tilde{n}_{4-}k_j(k_j - k_j'). \quad (73)$$

The angular average yields

$$\int d\Omega_{\boldsymbol{q}} \, d\Omega_{\boldsymbol{k}} \, d\Omega \, n_{1+}n_{2-}\tilde{n}_{3+}\tilde{n}_{4-}k_j(k_j - k_j')$$

$$= \frac{S_d^3}{d}k^2\big[I_{\ell=0}^2(a,b,c) - I_{\ell=1}^2(a,b,c)\big] \quad (74)$$

in terms of the functions $I_\ell(a,b,c)$ defined in Eqs. (55) and (56), and

$$\frac{1}{\tau_\parallel} = \frac{2S_d^3\beta n}{d(2\pi)^{2d}m^2 n_+ n_-} \int_0^\infty dq \, q^{d-1} \int_0^\infty dk \, k^{d+2}$$

$$\times \frac{d\sigma}{d\Omega}\big[I_0^2 - I_1^2\big]. \quad (75)$$

In the Boltzmann limit $T \gg T_F$ one finds $I_{\ell=0}^2 \to z_+ z_- \exp(-\beta\varepsilon_q/2)\exp(-2\beta\varepsilon_k)$ and $I_{\ell=1} \to 0$; hence (75) converges toward the transverse scattering rate (59) independent of polarization. Likewise, in the unpolarized case $n/n_+n_- \to 4/n$ and $I_1 \to 0$, and the longitudinal scattering time converges toward the transverse scattering time (66) for all temperatures.

## IV. RESULTS

### A. Three dimensions

Figure 1 shows the transverse and longitudinal spin diffusivity $D_\perp$ and $D_\parallel$ vs reduced temperature $T/T_F$ in three dimensions. Within kinetic theory the transverse and longitudinal diffusivities are equal in two limits: for unpolarized gases ($M = 0$) at arbitrary temperature, and in the Boltzmann limit $T \gg T_F$ for arbitrary polarization. We therefore focus our study on the polarized gas in the quantum degenerate regime where $D_\perp$ and $D_\parallel$ differ: as the polarization increases the transverse diffusivity $D_\perp$ decreases at low temperatures and reaches a finite value as $T \to 0$. This is in marked contrast
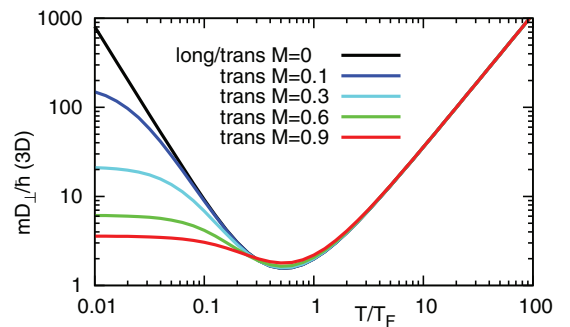


FIG. 1. (Color online) Transverse and longitudinal spin diffusivities $D_\perp$ and $D_\parallel$ vs reduced temperature $T/T_F$ for different polarizations $M$ (top $M = 0$ to bottom $M = 0.9$) for the unitary Fermi gas in three dimensions. The collision integral is computed using the vacuum $T$ matrix.
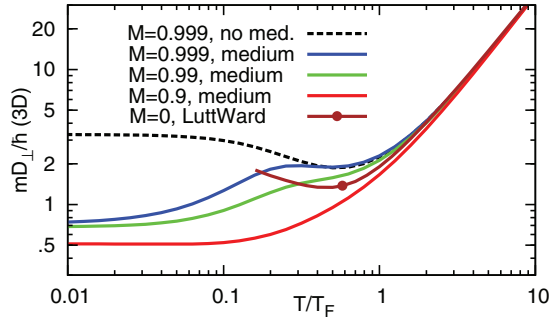
FIG. 2. (Color online) Transverse spin diffusivity $D_\perp$ vs reduced temperature $T/T_F$ including medium scattering (solid lines: top $M = 0.999$ to bottom $M = 0.9$). Due to increased scattering the medium diffusivity $D_\perp$ is lower than the vacuum diffusivity (dashed). For comparison, the Luttinger-Ward curve (with circle) for the unpolarized gas [23] above $T_c \simeq 0.16\,T_F$ includes not only medium scattering but also the renormalization of the fermionic spectral function.

to the longitudinal diffusivity, which due to Pauli blocking diverges as $D_\parallel \sim T^{-2}$ for a normal Fermi liquid.

In Fig. 1 the diffusivities have been computed with the vacuum scattering cross section, and the behavior agrees qualitatively with that in the Born approximation [10]. However, as explained in Sec. II A, in a systematic $1/N$ expansion to leading order one has to use the *medium* scattering cross section in combination with the thermodynamic functions of the free Fermi gas [31]. The many-body $T$ matrix (4) has to be computed numerically with one integral; hence the solution of the Boltzmann equation requires a three-dimensional integral. The resulting diffusivity $D_\perp$ is shown in Fig. 2. In the nondegenerate regime $T \gtrsim T_F$ the effect of medium scattering is still small. However, at lower temperatures the medium strongly enhances scattering and leads to a substantial suppression of the diffusivity, even more so away from the fully polarized limit. At the lowest temperatures $T \to 0$ the medium diffusivity still converges toward a finite value, as in the vacuum scattering case.

For large polarization above the Clogston-Chandrasekhar limit [33], the Fermi gas remains normal and the $T$ matrix is well defined down to zero temperature. For smaller polarization the $T$ matrix develops a pole associated with the phase transition, and the many-body $T$ matrix is reliable in the normal Fermi liquid phase above the phase transition. In the vicinity of the phase transition kinetic theory becomes inaccurate and one has to resort to more elaborate transport calculations using, for instance, the Luttinger-Ward framework based on the self-consistent $T$ matrix. For comparison, we plot the longitudinal spin diffusivity $D_\parallel(M = 0)$ (curve with circle) from a Luttinger-Ward calculation [23], which includes not only medium scattering but also the renormalization of spectral functions on equal footing, remaining regular down to $T_c \simeq 0.16\,T_F$.

Figure 3 shows the effect of spin rotation [1,12]: the spin current precesses around the effective molecular field with frequency $\Omega_{\mathrm{mf}}$, which results in a lower transverse diffusivity $D_\perp$. The molecular field frequency (72) of the unitary Fermi gas in the polaron limit $M \to 1$ reaches $\Omega_{\mathrm{mf}} \approx -1.2\,E_F$ for $T = 0$, which is twice the value of the chemical potential
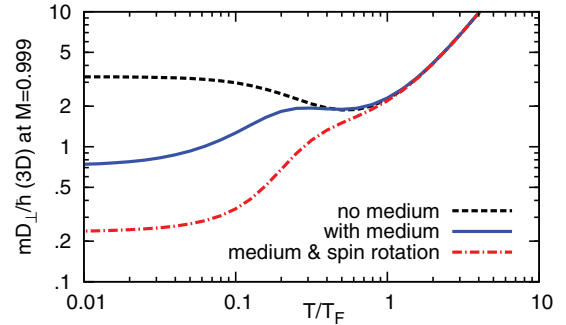


FIG. 3. (Color online) Spin-rotation effect on the transverse spin diffusivity $D_\perp$ vs reduced temperature $T/T_F$ for large polarization $M = 0.999$. Dashed line without medium scattering, solid line with medium effects, and dash-dotted line including the spin-rotation effect Eq. (37) with spin-rotation parameter $\mu = -\Omega_{\mathrm{mf}}\,\tau_\perp$, which further suppresses the diffusivity.

shift [34]. At large temperature, $\Omega_{\mathrm{mf}}$ decays as $T^{-2}$; hence $\mu = -\Omega_{\mathrm{mf}}\,\tau_\perp \sim T^{-3/2}$ and there is no spin rotation in the Boltzmann limit. Note that for the 3D unitary Fermi gas the *vacuum* $T$ matrix is purely imaginary at $a^{-1} = 0$ and leads to a vanishing molecular field; $\Omega_{\mathrm{mf}}$ is nonzero only for the *medium* $T$ matrix, which is used in Fig. 3. The full transverse spin diffusivity $D_\perp$ (dash-dotted line) is strongly suppressed at low temperatures but converges to the Boltzmann result at large temperature where the molecular field vanishes. This temperature dependence provides an experimentally accessible signature of the spin-rotation effect. Note that the external magnetic field $\gamma B$ does not affect the dynamics in the corotating frame [1].

In Fig. 4 the longitudinal spin diffusivity $D_\parallel$ is plotted vs polarization. At small polarization up to about 50% the diffusivity changes only slightly: it first increases and then drops for larger polarization. At very large polarization above 98%, it eventually saturates to a finite value in the limit $M \to 1$. This final value still depends on the temperature, roughly as $D_\parallel \sim 0.37\,(\hbar/m)\,(T/T_F)^{-1}$.

### B. Two dimensions

The spin diffusivity in 2D has recently attracted interest after spin-echo measurements in a transversely polarized spin
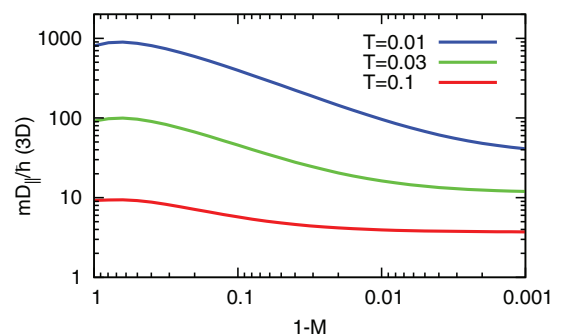


FIG. 4. (Color online) Longitudinal spin diffusivity $D_\parallel$ vs polarization $M$ at different temperatures $T/T_F$ (top $T/T_F = 0.01$ to bottom $T/T_F = 0.1$) for the 3D unitary Fermi gas (without medium scattering).
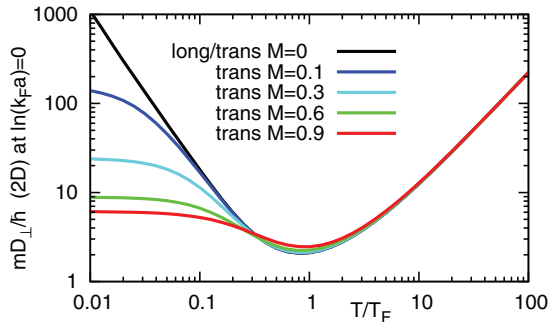
FIG. 5. (Color online) Transverse spin diffusivity $D_\perp$ vs reduced temperature $T/T_F$ for different polarizations $M$ (top $M=0$ to bottom $M=0.9$) for a strongly interacting 2D Fermi gas with interaction parameter $\ln(k_F a_{2D}) = 0$ (without medium scattering).

state in an ultracold gas of fermionic atoms [4]. The decay of magnetization over time allows one to infer the spin diffusivity, and very low values for $D_\perp$ have been found in the strongly interacting regime. In order to understand these results, we first compute the transverse and longitudinal spin diffusivities in 2D without medium scattering and find that they exhibit a qualitatively similar behavior as in the 3D case, as shown in Fig. 5.

However, the effect of medium scattering is even more pronounced in 2D than in 3D and can suppress the diffusivity by more than 1 order of magnitude at low temperature (see Fig. 6). For very large polarization $M = 0.999$ the diffusivity appears to saturate around $T/T_F = 0.1$ near $D_\perp \approx 5\hbar/m$ without medium scattering, and near $D_\perp \approx 0.1\hbar/m$ if the medium is included in the calculation. While Pauli blocking alone increases $D_\perp$ (dashed curve), the medium compensates this effect and leads to values of $D_\perp$ closer to the classical result (65) (dotted curve). The suppression of the diffusivity for smaller polarization signals the appearance of a superfluid density at low temperature, which would lead to a pole in the nonself-consistent $T$ matrix and a diverging collision integral [22].

The interaction dependence of the transverse diffusivity is shown in Fig. 7 for two values of the temperature in the quantum degenerate regime. At fixed polarization $M = 0.999$, the suppression by medium effects (solid vs dashed lines) is most pronounced in the strongly interacting region $-1 \lesssim \ln(k_F a_{2D}) \lesssim 1$, while at weak coupling the medium effects
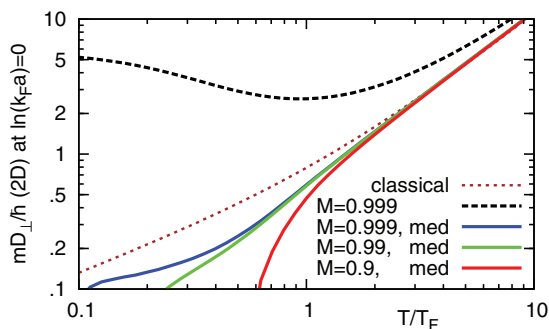


FIG. 6. (Color online) Transverse spin diffusivity $D_\perp$ vs reduced temperature $T/T_F$ in 2D, including medium scattering at strong interaction $\ln(k_F a_{2D}) = 0$ (solid lines: top $M = 0.999$ to bottom $M = 0.9$). The dashed line is for vacuum scattering, while the dotted curve illustrates the classical result (65) in the Boltzmann limit.
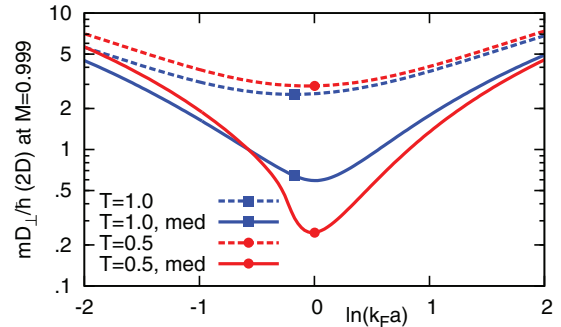


FIG. 7. (Color online) Transverse spin diffusivity $D_\perp$ vs interaction strength $\ln(k_F a_{2D})$ at fixed polarization $M = 0.999$ and temperatures $T/T_F = 1$ (blue/square), $T/T_F = 0.5$ (red/circle). The dashed lines denote the diffusivity without medium effects, while the solid lines include medium scattering.

lower the diffusivity only slightly. The values of $D_\perp$ in Fig. 7 come close to $D_\perp = 0.25(3)\hbar/m$, measured in a recent 2D spin-echo experiment [4], although the measured minimum around $\ln(k_F a_{2D}) = 0$ is more shallow than in our calculation.

In order to make a detailed comparison of our transport calculation for the homogeneous system with experiments in a trap geometry, it would be useful to measure the diffusivity for evolution times shorter than the trap period in order to minimize the effects of the trap. Measuring the temperature dependence of the diffusivity would also provide a much more sensitive comparison of theory and experiment, in particular, regarding the spin-rotation effect displayed in Fig. 3.

## V. CONCLUSION

We have presented a kinetic theory for transverse and longitudinal spin diffusion in strongly interacting Fermi gases in two and three dimensions based on the many-body $T$ matrix. We find a significant suppression of the spin diffusivities at low temperatures and strong coupling due to medium scattering beyond the Born approximation. The results are consistent with the very low transverse spin diffusivity $D_\perp$ observed in a recent 2D spin-echo experiment [4] at strong interaction. Our analysis includes the Leggett-Rice effect of spin rotation by a molecular field [1], which further lowers the transverse diffusion coefficient of a polarized gas. It will be interesting to study the role of mean-field corrections to the quasiparticle dispersion relation [32] in a future work.

For small polarization below the Clogston-Chandrasekhar limit, the interacting Fermi gas exhibits a phase transition toward superfluidity and the ladder approximation for the $T$ matrix may have to be amended by particle-hole fluctuations near the transition. In this case it would be worthwhile to compute transverse spin transport also using other theoretical approaches which go beyond a quasiparticle description, such as the Luttinger-Ward [23] or Monte Carlo methods [24], but we expect that the qualitative features will be similar.

[1] A. J. Leggett, J. Phys. C **3**, 448 (1970).

[2] *Semiconductor Spintronics and Quantum Computation*, edited by D. D. Awschalom, D. Loss, and N. Samarth (Springer, New York, 2002).

[3] A. Sommer, M. Ku, G. Roati, and M. W. Zwierlein, Nature (London) **472**, 201 (2011).

[4] M. Koschorreck, D. Pertot, E. Vogt, and M. Köhl, Nat. Phys. **9**, 405 (2013).

[5] L. D. Landau, Zh. Eksp. Teor. Fiz. **30**, 1058 (1956) [Sov. Phys. JETP **3**, 920 (1957)]; V. P. Silin, Zh. Eksp. Teor. Fiz. **33**, 1227 (1957) [Sov. Phys. JETP **6**, 945 (1958)].

[6] C. Lhuillier and F. Laloë, J. Phys. (France) **43**, 197 (1982).

[7] A. E. Meyerovich, Phys. Lett. A **107**, 177 (1985).

[8] J. W. Jeon and W. J. Mullin, J. Low Temp. Phys. **67**, 421 (1987).

[9] J. W. Jeon and W. J. Mullin, J. Phys. (France) **49**, 1691 (1988).

[10] J. W. Jeon and W. J. Mullin, Phys. Rev. Lett. **62**, 2691 (1989).

[11] A. E. Ruckenstein and L. P. Lévy, Phys. Rev. B **39**, 183 (1989).

[12] W. J. Mullin and J. W. Jeon, J. Low Temp. Phys. **88**, 433 (1992).

[13] A. E. Meyerovich and K. A. Musaelian, J. Low Temp. Phys. **89**, 781 (1992); **94**, 249 (1994); **95**, 789 (1994); A. E. Meyerovich, S. Stepaniants, and F. Laloë, Phys. Rev. B **52**, 6808 (1995).

[14] W. J. Mullin and R. J. Ragan, Phys. Rev. A **74**, 043607 (2006).

[15] I. Bloch, J. Dalibard, and W. Zwerger, Rev. Mod. Phys. **80**, 885 (2008).

[16] T. Schäfer and D. Teaney, Rep. Prog. Phys. **72**, 126001 (2009); C. Cao, E. Elliott, J. Joseph, H. Wu, J. Petricka, T. Schäfer, and J. E. Thomas, Science **331**, 58 (2011).

[17] T. Enss, R. Haussmann, and W. Zwerger, Ann. Phys. (NY) **326**, 770 (2011).

[18] G. Wlazłowski, P. Magierski, and J. E. Drut, Phys. Rev. Lett. **109**, 020406 (2012).

[19] R. A. Duine, M. Polini, H. T. C. Stoof, and G. Vignale, Phys. Rev. Lett. **104**, 220403 (2010).

[20] G. M. Bruun, New J. Phys. **13**, 035005 (2011).

[21] G. M. Bruun, Phys. Rev. A **85**, 013636 (2012).

[22] T. Enss, C. Küppersbusch, and L. Fritz, Phys. Rev. A **86**, 013617 (2012).

[23] T. Enss and R. Haussmann, Phys. Rev. Lett. **109**, 195303 (2012).

[24] G. Wlazłowski, P. Magierski, J. E. Drut, A. Bulgac, and K. J. Roche, Phys. Rev. Lett. **110**, 090401 (2013).

[25] T. Enss, Eur. Phys. J. Spec. Topics **217**, 169 (2013).

[26] P. Nozières and S. Schmitt-Rink, J. Low Temp. Phys. **59**, 195 (1985).

[27] S. K. Adhikari, Am. J. Phys. **54**, 362 (1986); J. R. Engelbrecht and M. Randeria, Phys. Rev. B **45**, 12419 (1992).

[28] D. S. Petrov and G. V. Shlyapnikov, Phys. Rev. A **64**, 012706 (2001).

[29] M. J. H. Ku, A. T. Sommer, L. W. Cheuk, and M. W. Zwierlein, Science **335**, 563 (2012).

[30] P. Nikolić and S. Sachdev, Phys. Rev. A **75**, 033608 (2007); M. Y. Veillette, D. E. Sheehy, and L. Radzihovsky, *ibid.* **75**, 043614 (2007).

[31] T. Enss, Phys. Rev. A **86**, 013616 (2012).

[32] S. Chiacchiera, T. Lepers, D. Davesne, and M. Urban, Phys. Rev. A **79**, 033613 (2009).

[33] C. Lobo, A. Recati, S. Giorgini, and S. Stringari, Phys. Rev. Lett. **97**, 200403 (2006); F. Chevy and C. Salomon, in *The BCS-BEC Crossover and the Unitary Fermi Gas*, edited by W. Zwerger (Springer, Berlin, 2012), p. 407.

[34] R. Schmidt and T. Enss, Phys. Rev. A **83**, 063620 (2011); R. Schmidt, T. Enss, V. Pietilä, and E. Demler, *ibid.* **85**, 021602(R) (2012).

[35] T. Schäfer, Phys. Rev. A **85**, 033623 (2012).